Inorganic Chemistry

Article

pubs.acs.org/IC

A Synthesis and Crystal Chemical Study of the Fast Ion Conductor $Li_{7-3x}Ga_xLa_3Zr_2O_{12}$ with $x = 0.08$ to 0.84

Daniel Rettenwander,*[,†] Charles A. Geiger,[†] Martina Tribus,[‡] Peter Tropper,[‡] and Georg Amthauer[†]

[†]Department of Materials Science and Physics, University of Salzburg, Hellbrunnerstrasse 34, A-5020 Salzburg, Austria

[‡]Institute of Mineralogy and Petrography, Faculty of Geo- and Atmospheric Sciences, University of Innsbruck, Innrain 52, A-6020 Innsbruck, Austria

ABSTRACT: Fast-conducting phase-pure cubic Ga-bearing $Li_7La_3Zr_2O_{12}$ was obtained using solid-state synthesis methods with 0.08 to 0.52 Ga^{3+} pfu in the garnet. An upper limit of 0.72 Ga^{3+} pfu in garnet was obtained, but the synthesis was accompanied by small amounts of $La_2Zr_2O_{12}$ and $LiGaO_3$. The synthetic products were characterized by X-ray powder diffraction, electron microprobe and SEM analyses, ICP-OES measurements, and ^{71}Ga MAS NMR spectroscopy. The unit-cell parameter, a_0, of the various garnets does not vary significantly as a function of Ga^{3+} content, with a value of about 12.984(4) Å. Full chemical analyses for the solid solutions were obtained giving: $Li_{7.08}Ga_{0.06}La_{2.93}Zr_{2.02}O_{12}$, $Li_{6.50}Ga_{0.15}La_{2.96}Zr_{2.05}O_{12}$, $Li_{6.48}Ga_{0.23}La_{2.93}Zr_{2.04}O_{12}$, $Li_{5.93}Ga_{0.36}La_{2.94}Zr_{2.01}O_{12}$, $Li_{5.38}Ga_{0.53}La_{2.96}Zr_{1.99}O_{12}$, $Li_{4.82}Ga_{0.60}La_{2.96}Zr_{2.00}O_{12}$, and $Li_{4.53}Ga_{0.72}La_{2.94}Zr_{1.98}O_{12}$. The NMR spectra are interpreted as indicating that Ga^{3+} mainly occurs in a distorted 4-fold coordinated environment that probably corresponds to the general 96*h* crystallographic site of garnet.

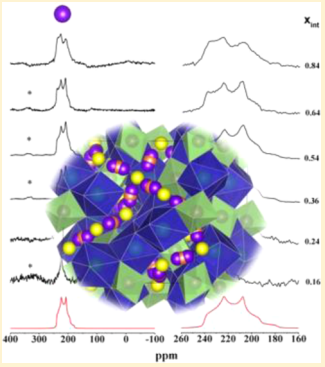

INTRODUCTION

Research has shown that Al-bearing $Li_7La_3Zr_2O_{12}$ (LLZO) with a cubic garnet structure has high ion conductivity (approximately 10^{-4} S·cm^{-1}).[1] At room temperature, end-member LLZO is tetragonal ($I4_1/acd$) and it has a lower conductivity compared to the "high temperature" cubic modification ($Ia\text{-}3d$).[2] The tetragonal phase has a fully ordered arrangement of Li^+ ions. It has been proposed that by doping LLZO with supervalent cations the cubic structure is stabilized by introducing vacancies at the Li positions, which act to increase the entropy and reduce the free energy.[3] The stabilization of cubic LLZO through Al^{3+} was first reported in 2011[4,5] and confirmed many times thereafter.[6−17] Attention has since been directed also at other dopant cations. Because gallium is located directly below aluminum in the periodic table, it should show similar crystal-chemical behavior as Al^{3+} in LLZO. Indeed, the stabilization of cubic LLZO through Ga^{3+} has been reported.[17−19]

In spite of the amount of recent study that has been made on the LLZO group of phases, certain aspects are still not understood. Emphasis has been placed on measuring Li-ion conductivity often at the expense of careful compositional and crystal-chemical characterization of the garnet under consideration. The latter are important, if not essential, in order to understand the precise stability and conductivity behavior of LLZO. In terms of Ga-bearing LLZO, there is no information about the amount of Ga^{3+} that can be incorporated and its site distribution with the garnet structure.

To obtain a more detailed understanding of the role of super valent cations in LLZO, we synthesized a series of $Li_{7-3x}Ga^{3+}{}_xLa_3Zr_2O_{12}$ garnets and carefully characterized them chemically and structurally. Characterization was done using X-ray powder diffraction (XRPD) measurements, electron microprobe analysis (EMPA), inductively coupled plasma optical emission spectroscopy (ICP-OES) measurements, and ^{71}Ga magic angle spinning (MAS) nuclear magnetic resonance (NMR) spectroscopy.

EXPERIMENTAL SECTION

A series of $Li_{7-3x}Ga^{3+}{}_xLa_3Zr_2O_{12}$ garnets with intended mole fractions of Ga^{3+} (x_{int}) of 0.08−0.84 pfu was synthesized by high-temperature sintering in air. The starting materials were Li_2CO_3 (99%, Merck), La_2O_3 (99.99%, Aldrich), ZrO_2 (99.0%, Aldrich), and Ga_2O_3 (99.0%, Aldrich). To begin, the starting materials were weighed out in their intended stoichiometric proportions together with an excess of 10 wt % Li_2CO_3 to compensate for Li_2O loss during synthesis. After intimate mixing in a ball mill for 8 h, the starting mix was cold-pressed into pellets of 10 mm diameter and 5 mm height. The pellets were placed in a Pt crucible and heated at a rate of 5 °C/min to 900 °C and calcinated for 4 h. The resulting pellets were then removed from the oven, were allowed to cool, and were ground for 15 min and pressed again into pellets. The final sintering step was done at 1050 °C for 17 h in air. A small amount of a given compacted sintered pellet, taken from the middle of the pellet, was ground and used for the XRPD, ^{71}Ga MAS NMR, and ICP-OES measurements. A polycrystalline chip was used for microprobe analysis.

XRPD measurements were performed with Cu Kα radiation using a Siemens D8 diffractometer. This was done to characterize the synthetic products in terms of the phases present and to determine the symmetry and unit-cell dimension of the garnet. Data were collected between 10° and 70° 2θ. The unit-cell lattice parameter, a_0, and grain size were determined by Rietveld refinement using the program Topas V2.1 (Company Bruker).

Received: April 8, 2014
Published: May 29, 2014

   dx.doi.org/10.1021/ic500803h | *Inorg. Chem.* 2014, 53, 6264−6269

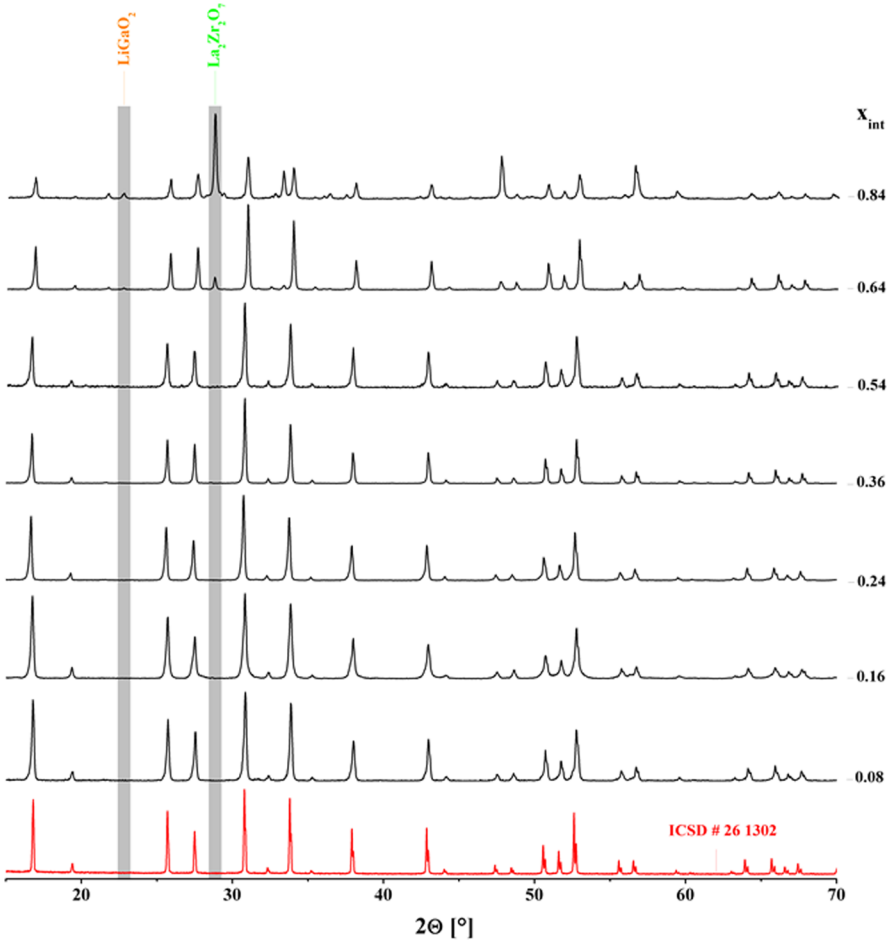

Figure 1. XRPD patterns of $Li_{7-3x}Ga_xLa_3Zr_2O_{12}$ garnet solid solutions with x_{int} = 0.08−0.84. The diffraction pattern (red) of cubic $Li_{7-3x}Al_xLa_3Zr_2O_{12}$ with x = 0.24 is shown for comparison. Only the strongest reflections of non-garnet phases are observed at high Ga^{3+} contents and their positions are highlighted with a gray background.

EMPA was done using a JEOL JXA 8100 Superprobe at the Institute of Mineralogy and Petrography at the University of Innsbruck. Small polycrystalline chips, taken from the larger sintered pellets, were embedded in an epoxy holder, and the surface was ground and then polished using diamond paste. Special attention was made with regard to grain sizes, grain boundaries, and textures during analysis. Back-scattered electron (BSE) images were taken to identify small amounts of non-garnet phases. Wavelength-dispersive (WDS) measurements for the elements La, Zr, and Ga were undertaken to characterize the synthetic products in terms of their composition and chemical homogeneity. Analytical measuring conditions were 15 kV accelerating voltage and a 10 nA beam current. The following synthetic standards were used: GaAs (99.99%, Aldrich) for Ga, La-phosphate, LaP_5O_{14}, for La, and zircon, $ZrSiO_4$, for Zr. Measuring times were 20 s at the peak maximum and 10 s for the lower and upper peak background. Twenty point measurements, made on five different garnet grains, were performed to obtain representative compositions for each garnet composition.

ICP-OES measurements, using a Horiba Jobin Yvon Ultima 2 device, were made to determine the Li contents at the University of Ulm, Germany. About 50 mg of garnet, taken from a sintered pellet, were divided into two batches in order to be able to determine the analytical reproducibility. The samples were prepared by placing 15 mg of garnet in 2 mL of aqua regia (HCl + HNO_3), followed by heating to ensure dissolution of the garnet. Deionized water was then added to obtain 20 mL of solution. One mL aliqouts were used for the ICP-OES measurements.

^{71}Ga MAS NMR spectra were recorded at room temperature on the same Ga^{3+}-bearing samples that were characterized by XRPD, EMPA, and ICP-OES measurements using a Bruker ASX 400 spectrometer at Ruhr University in Bochum, Germany. MAS NMR spectra were collected at 122 MHz (9.4 T) with a spinning rate of 12.5 kHz using a 4 mm MAS probe. Spectra were recorded with a single pulse sequence; the pulse length was 0.6 μs. The spectral width was 125 kHz corresponding to a radio frequency tip angle of about 15 ± 5°. The signal-to-noise ratio was optimized by a pulse delay of 0.4 s using full relaxation for short pulses. Line broadening of 100 Hz was applied and the first 4−8 points of 1 k measured free induction decay (FID) points were removed because of the strong distortion and low signal. The count of the spectral points was 8 k. Typically, about 10^6 scans were acquired for samples with x_{int} < 0.36 and about 2 × 10^5 for samples with x_{int} ≥ 0.24. Line shapes were simulated using the STARS simulation package (Varian), with manual adjustment of parameters to match the quadrupolar line shapes typical of the spectra for the samples with x_{int} = 0.24 to x_{int} = 0.64. The ^{71}Ga chemical shifts are reported relative to aqueous 1 M $Ga(NO_3)_3$.

RESULTS

Garnet Composition and Lattice Constant. The XRPD patterns of the various $Li_{7-3x}Ga_xLa_3Zr_2O_{12}$ garnets with x_{int} = 0.08, 0.16, 0.24, 0.36, 0.54, 0.64, and 0.84 are shown in Figure 1, together with the pattern of $Li_{7-x}Al_xLa_3Zr_2O_{12}$ with x = 0.24 (ICSD no. 261302). All garnet compositions exhibit reflections indicating cubic symmetry. There are no indications of reflection splitting indicating a tetragonal garnet phase. All diffraction patterns of garnet with x_{int} from 0.08 to 0.54 do not show the presence of any other phase. In the diffraction pattern

dx.doi.org/10.1021/ic500803h | Inorg. Chem. 2014, 53, 6264−6269

of the sample with x_{int} = 0.64, just one weak reflection is observed and it can be assigned to $La_2Zr_2O_7$ occurring at roughly the 1% level. For the garnet with x_{int} = 0.84, about 4% $LiGaO_2$ and 6% $La_2Zr_2O_7$ are calculated from Rietveld analysis. The unit-cell constant, a_0, and a determination of the amounts of the different phases were evaluated by Rietveld analysis. The results are summarized in Table 1 and shown in Figure 2. The

Table 1. Unit-Cell Parameter of $Li_{7-3x}Ga_xLa_3Zr_2O_{12}$ with x_{int} = 0.08−0.84 and the Amount of Phases in the Different Syntheses Obtained by Rietveld Refinement

x_{int}	a_0 [Å]	LLZO [%]	$La_2Zr_2O_7$ [%]	$LiGaO_2$ [%]
0.08	13.034(6)	100	0	0
0.16	12.981(2)	100	0	0
0.24	12.971(4)	100	0	0
0.36	12.969(1)	100	0	0
0.54	12.979(9)	100	0	0
0.64	12.973(2)	>99	<1	0
0.84	12.979(5)	90	6	4

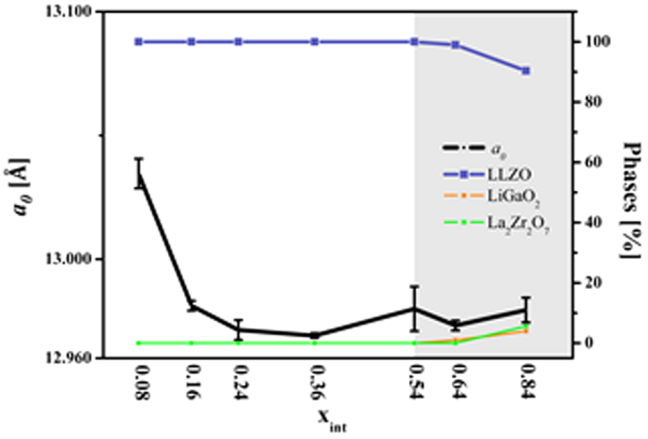

Figure 2. Lattice parameter, a_o, and amount of phases obtained in the synthesis experiments as a function of the intended Ga^{3+} concentration in LLZO.

unit-cell constant of garnet with x_{int} = 0.08 is 13.034(6) Å, and this value decreases slightly to 12.971(4) Å for garnet with x_{int} = 0.24. More Ga-rich garnets have a similar a_0 value of 12.979(5) for the sample with x_{int} = 0.84. The a_0 values are similar to Al-bearing LLZO with a_0 = 12.975(1) Å or to Fe-bearing LLZO with a_0 = 12.986(1) Å.[5,20]

The X-ray reflections for Ga-bearing LLZO are broader than those of Al-bearing LLZO and increase, especially at small 2θ, with increasing Ga^{3+} concentration.

Phase Identification and Compositional Homogeneity (EMPA). BSE images of polycrystalline chips made with the EPMA are shown in Figure 3. Examination reveals only garnet and no other phases for compositions from x_{int} = 0.08 up to x_{int} = 0.54. Garnet crystal diameters are ∼10 μm. $La_2Zr_2O_7$ could be identified in the sample with x_{int} = 0.64 pfu and $La_2Zr_2O_7$ and $LiGaO_3$ in the sample with x_{int} = 0.84 pfu. The density of the various samples appears to increase with increasing Ga^{3+} content.

Chemical Composition (EMPA and ICP-OES). The chemical analyses obtained using EMPA and ICP-OES measurements are reported in Tables 2 and 3 and shown in Figure 4. Ga, La, and Zr were measured by electron microprobe. Because Li cannot be measured by electron

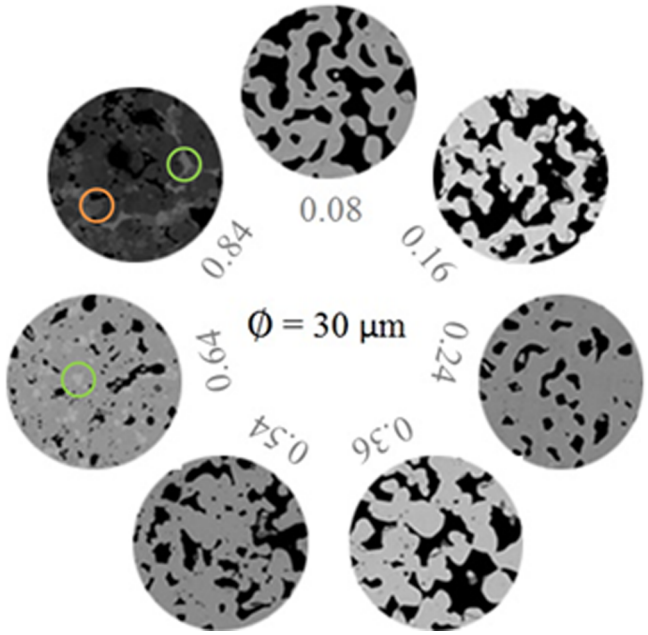

Figure 3. BSE images of the various $Li_{7-3x}Ga_xLa_3Zr_2O_{12}$ samples with x_{int} = 0.08−0.84. Only garnet crystals are observed from x_{int} = 0.08 to x_{int} = 0.54. The dark regions are holes in the surface of the sample. The orange circle shows the phase $LiGaO_3$, and green circles show $La_2Zr_2O_7$. The diameter of each total sample circle is 30 μm.

Table 2. EMPA (Ga, La, Zr) and ICP-OES (Li) Results for $Li_{7-3x}Ga_xLa_3Zr_2O_{12}$ with x_{int} = 0.08−0.84 in wt %

x_{int}	Ga_2O_3	Li_2O[a]	La_2O_3	ZrO_2	total
0.08	0.73(4)	11.83	57.16(12)	29.79(35)	99.51(51)
0.16	1.83(8)	10.49	56.49(70)	29.88(35)	98.69(14)
0.24	2.78(8)	10.42	56.57(23)	29.63(35)	99.40(50)
0.36	4.31(10)	9.90	55.86(57)	29.11(35)	99.18(10)
0.54	6.15(4)	9.06	55.91(19)	28.59(35)	99.71(33)
0.64	6.92(11)	8.37[b]	54.98(78)	28.65(17)	100.00
0.84	8.33(9)	7.80[b]	54.65(73)	28.29(17)	100.00

[a]Measured by ICP-OES. Data were normalized to 100 wt % for the elemental oxides. Values in brackets are the standard deviation based on 20 point analyses. [b]Values were calculated according to $[Li_2O] = 100 - [Ga_2O_3] - [La_2O_3] - [ZrO_2]$.

Table 3. Crystal Chemical Formulae of the $Li_{7-3x}Ga_xLa_3Zr_2O_{12}$ Samples[a]

x_{int}	Ga^{3+}	Li^+	La^{3+}	Zr^{4+}
0.08	0.06(1)	7.08	2.93(1)	2.02(2)
0.16	0.15(1)	6.50	2.96(3)	2.05(3)
0.24	0.23(1)	6.48	2.93(2)	2.04(2)
0.36	0.36(1)	5.93	2.94(1)	2.01(3)
0.54	0.53(2)	5.38	2.96(3)	1.99(2)
0.64	0.60(2)	4.82	2.96(1)	2.00(1)
0.84	0.72(1)	4.53	2.94(1)	1.98(2)

[a]Calculated using the values given in Table 2 on the basis of 12 oxygen atoms per formula unit [pfu].

microprobe analysis, the Li_2O content of those syntheses that yielded only garnet was measured by ICP-OES.

Crystal Chemical Formula. The measured Ga^{3+} concentrations of the various single phase garnet samples (x_{obs}) are close to the nominal values of the starting material: x_{int} = 0.08 → x_{obs} = 0.06(1), x_{int} = 0.16 → x_{obs} = 0.15(1), x_{int} = 0.24 → x_{obs}

dx.doi.org/10.1021/ic500803h | Inorg. Chem. 2014, 53, 6264−6269

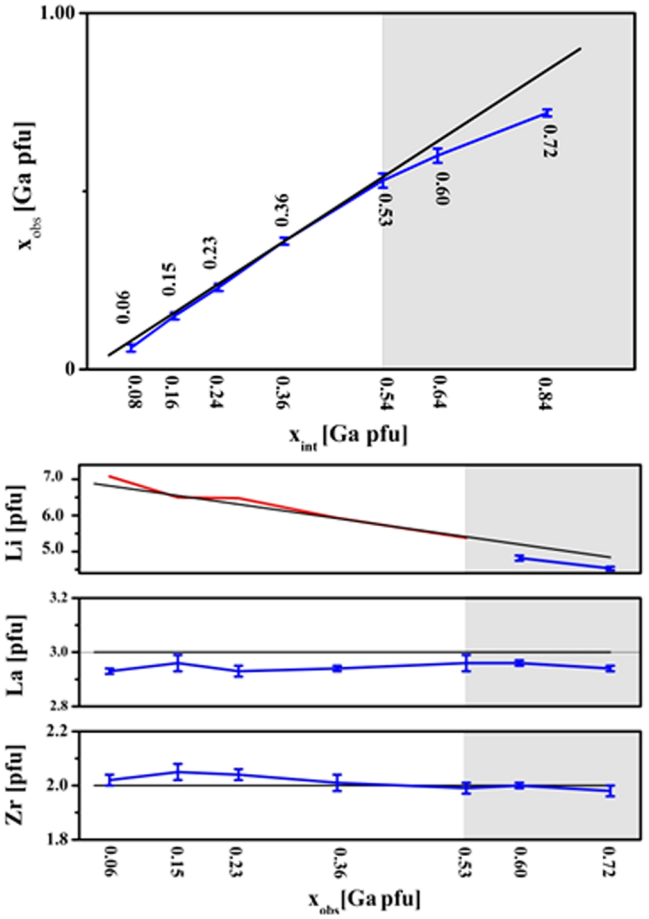

Figure 4. Plot of measured vs intended compositions for $Li_{7-3x}Ga_xLa_3Zr_2O_{12}$ with x_{int} = 0.08−0.84. The black lines correspond to intended garnet compositions, the blue lines to the EMPA measured values, and the red line to the ICP-OES measurements. The gray area corresponds to those bulk compositions where non-garnet phases are present in the synthetic product.

= 0.23(1), x_{int} = 0.36 → x_{obs} = 0.36(1), and x_{int} = 0.54 → x_{obs} = 0.53(2). When additional non-garnet phases are present, the Ga^{3+} content in LLZO is lower than that in the starting material: x_{int} = 0.64 → x_{obs} = 0.60(2) and x_{int} = 0.84 → x_{obs} = 0.72(1). The Li content measured with ICP-OES (Li_{obs}) agrees satisfactorily with the Li content (Li_{theo}) of the starting material: x_{int} = 0.08, Li_{theo} = 6.82 → Li_{obs} = 7.08; x_{int} = 0.16, Li_{theo} = 6.55 → Li_{obs} = 6.50; x_{int} = 0.24, Li_{theo} = 6.31 → Li_{obs} = 6.48; x_{int} = 0.36, Li_{theo} = 5.92 → Li_{obs} = 5.93; and x_{int} = 0.54, Li_{theo} = 5.41 → Li_{obs} = 5.38. For more Ga-rich samples having additional non-garnet phases, the Li content was calculated based on [Li_2O] = 100 − [Ga_2O_3] − [La_2O_3] − [ZrO2] and gives for x_{int} = 0.64, Li_{theo} = 5.08 → Li_{obs} = 4.82(7), and x_{int} = 0.84, Li_{theo} = 5.41 → Li_{obs} = 4.53(5).

Figure 4 shows that measured La and Zr contents are close to their stoichiometric values of 3.0 and 2.0, respectively, with a maximum deviation of ∼2% pfu (considering the standard deviations). The calculated chemical formulas of the various garnet solid solutions using the EMPA and ICP-OES results are

x_{int} = 0.08: $Li_{7.08}Ga_{0.06}La_{2.93}Zr_{2.02}O_{12}$

x_{int} = 0.16: $Li_{6.50}Ga_{0.15}La_{2.96}Zr_{2.05}O_{12}$

x_{int} = 0.24: $Li_{6.48}Ga_{0.23}La_{2.93}Zr_{2.04}O_{12}$

x_{int} = 0.36: $Li_{5.93}Ga_{0.36}La_{2.94}Zr_{2.01}O_{12}$, and

x_{int} = 0.54: $Li_{5.38}Ga_{0.53}La_{2.96}Zr_{1.99}O_{12}$

The chemical formulas of the garnet solid solutions with additional non-garnet phases in the synthetic products are

x_{int} = 0.64: $Li_{4.82}Ga_{0.60}La_{2.96}Zr_{2.00}O_{12}$and

x_{int} = 0.84: $Li_{4.53}Ga_{0.72}La_{2.94}Zr_{1.98}O_{12}$

We note that the La^{3+} content in all LLZO samples appears to be slightly too low. This may possibly reflect a systematic analytical artifact related to the La standard used or in the correction procedure. Other reasons could be a possible substitution of La^{3+} by Li^+ or Zr^{4+} at the dodecahedral site.

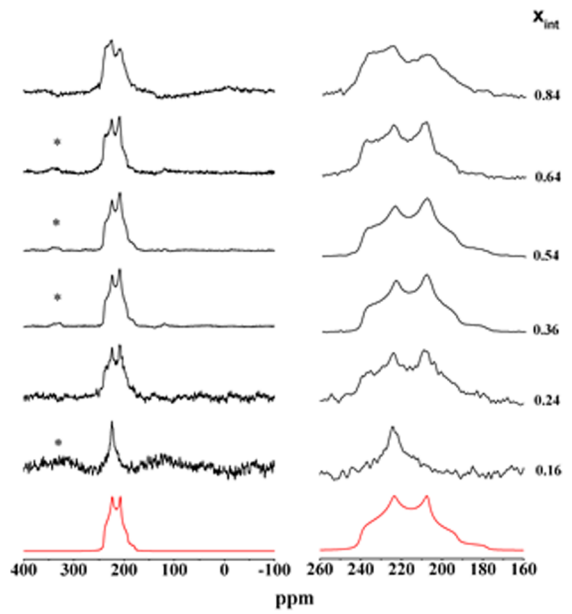

Figure 5. ^{71}Ga MAS NMR spectra of $Li_{7-3x}Ga^{3+}{}_xLa_3Zr_2O_{12}$ garnets with x_{int} = 0.08−0.84. Asterisks (*) mark spinning side bands. The spectra on the right are shown over a smaller range of chemical shift values. The spectrum shown in red is simulated for the sample with x_{int} = 0.36.

^{71}Ga MAS NMR Spectra. Spectra for the samples with x_{int} = 0.16, 0.24, 0.36, 0.54, 0.64, and 0.84 are shown in Figure 5. ^{71}Ga (spin quantum number I = 3/2, natural abundance 39.6%) is a quadrupole nucleus; the interaction of its rather large quadrupole moment (Q = 10.7 × 10^{-30} m^2) with the surrounding electric field gradient results in a central line that is perturbed by second-order effects. Their shape can be simulated well with a single set of NMR parameters, namely an isotropic chemical shift, δ, of 244(2) ppm, a quadrupolar coupling constant, C_Q, of 4.0(2) MHz, and an asymmetry parameter, η_Q, of 0.46(3). The spectrum of the sample with x_{int} = 0.84, which has a slightly different line shape than those in the spectra of the other garnets (Figure 5), also has a NMR resonance with the major component at δ = 244(2) ppm. The spectra for samples with Ga^{3+} contents, x_{int} ≥ 0.36, show the best signal to background ratios.

We interpret these spectra, as well as that for x_{int} = 0.24, as indicating that Ga^{3+} is located at a single structural site in LLZO. The observed δ values indicate Ga^{3+} with 4-fold

dx.doi.org/10.1021/ic500803h | Inorg. Chem. 2014, 53, 6264−6269

coordination.[21] The rather large η_Q value indicates that Ga^{3+} is located at a structural site with no axial symmetry. This might exclude the special crystallographic tetrahedrally coordinated site 24*d* in garnet with site symmetry −4 from consideration. It should be noted, however, that the local symmetry around Ga^{3+} could be lower than that determined by diffraction measurements. The interpretation of the spectrum of the sample with x_{int} = 0.16 is difficult because the single resonance could be assigned to a small amount of Ga^{3+} located at a site with a smaller C_Q. The spectrum of the sample with x_{int} = 0.84 could indicate the presence of two Ga-bearing phases. The major phase is clearly Ga-bearing LLZO and the second possibly minor $LiGaO_2$. The latter was identified by XRPD measurements. $LiGaO_2$ has similar NMR parameters of δ = 242(2), C_Q = 3.89(5), and η_Q = 0.37(2) and line shape as Ga-bearing LLZO.[21] This spectrum could represent the superposition of a garnet phase and $LiGaO_2$. A similar situation may be shown in the spectrum with x_{int} = 0.64, although no $LiGaO_2$ was detected by XRPD or EPMA.

DISCUSSION

The main goal of this study is to investigate the degree of solid solution and crystal-chemical properties of Ga-bearing LLZO garnet. To understand our discussion, we provide a short description of the crystal structure of cubic LLZO garnet.

$Li_7La_3Zr_2O_{12}$ with cubic symmetry *Ia*-3*d* has O^{2-} ions that are located at general crystallographic positions, 96*h*. They form an oxygen-ion framework with interstices occupied by the La^{3+} at the 8-fold coordinated position 24*c* (point symmetry 222) and by Zr^{4+} at the 6-fold coordinated position 16*a* (point symmetry −3). Li^+ is partially located at the 4-fold coordinated 24*d* position (point symmetry −4) as well as the 6-fold coordinated 48*g* positions (point symmetry 2) and a "4-fold" coordinated 96*h* position (point symmetry 1). The latter two sites are empty in the conventional garnet structure.[22] The crystal structure is illustrated in Figure 6.

Allen et al. were the first to study Ga^{3+} incorporation in Li-oxide garnet.[23] They investigated the conductivity behavior of a garnet of composition $Li_{6.75}La_{3.00}Zr_{1.75}Ta_{0.25}0_{12.00}$ and two compositions with Ga^{3+} or Al^{3+} doping. The samples were prepared from a coprecipitated precursor and calcinated by solid-state sintering. Garnet without Ga^{3+} or Al^{3+} showed a slightly higher Li-ion conductivity, σ, at room temperature (σ = 8.7 × 10^{-4} S·cm^{-1}) than garnet of composition $Li_{6.15}La_{3.00}Zr_{1.75}Ta_{0.25}Ga_{0.20}O_{12.00}$ (σ = 4.1 × 10^{-4} S·cm^{-1}) and $Li_{6.15}La_{3.00}Zr_{1.75}Ta_{0.25}Al_{0.20}O_{12.00}$ (σ = 3.7 × 10^{-4} S·cm^{-1}). They proposed that Ga^{3+} mainly occupies the 96*h* site, whereas Al^{3+} is located at 24*d* based on considering the work of Geller et al., who reported that Ga^{3+} preferred 6-fold coordination in garnet (16*a*).[24] Howard et al. synthesized cubic garnet of composition $Li_{5.50}Ga_{0.50}La_3Zr_2O_{12}$ using solid-state sintering methods.[17] A ^{71}Ga MAS NMR spectrum showed a single resonance with a chemical shift of ∼221 ppm. They proposed, in contrast to Allen et al., that Ga^{3+} occupies the tetrahedrally coordinated special crystallographic 24*d* site. A third investigation of Ga-bearing LLZO garnet was undertaken by El Shinawi and Janek.[18] Here, a series of $Li_{7-x}Ga_xLa_3Zr_2O_{12}$ garnets, synthesized using sol−gel methods, with *x* = 0.1, 0.2, 0.3, 0.4, 0.5, and 1.0, were prepared. XRPD analysis indicated the presence of additional non-garnet phases for LLZO compositions with *x* = 0.1, 0.2, 0.5, and 1.0 Ga^{3+} pfu. They measured only small Ga^{3+} contents directly in garnet. Instead, most Ga^{3+} was concentrated at grain boundaries. The non-garnet phases were: (i) $La_2Zr_2O_7$, which was present in compositions with *x* = 0.1, 0.2, 0.5, and 1.0 Ga^{3+} pfu, and (ii) $LiGaO_2$, together with another La^{3+}- or Zr^{4+}-containing phase, for samples with *x* > 0.5 Ga^{3+} pfu. In terms of the garnet, they observed increasing ion conductivity with increasing Ga^{3+} content.

Our work demonstrates that single phase Ga-bearing LLZO can be synthesized with up to *x* = 0.53 Ga^{3+} pfu. A Ga^{3+} content of up to *x* = 0.72 Ga^{3+} pfu in garnet can be obtained, but herein it is associated with small amounts of additional non-garnet phases. Our results differ from the unspecified minor amount of Ga^{3+} incorporated in LLZO as observed by El Shinawi and Janek.[18] We think this reflects the different sample preparation and synthesis route. For example, in the case of the synthesis of Al-bearing LLZO it has been shown that $LiAlO_2$ can occur at grain boundaries or that the Al^{3+} is incorporated in the garnet, depending upon the exact synthesis conditions.[25]

Previous studies of Ga-bearing Li-oxide garnet have proposed that Ga^{3+} can reside at 24*d*[17] or at 96*h*[24]. We think that the large η_Q value that is greater than 0.40, together with the relatively large ionic radius of Ga^{3+} ($r^{[6]}$ = 0.62 Å),[26] argues for local "4-fold" coordination. We think that this occurs at the 96*h* site (site symmetry: 1 ⇒ $\eta_Q \neq 0$). Both observations argue against the proposal that Ga^{3+} is located at the "standard garnet" tetrahedrally coordinated 24*d* site (site symmetry: −4 ⇒ η_Q = 0).

To understand the behavior of Ga^{3+} better, one can also consider the case of Al^{3+} in LLZO garnet. The latter are better understood in terms of their crystal chemistry, and ^{27}Al NMR spectra and can be used as a guide to interpret our ^{71}Ga NMR results. It has been proposed that a relationship between ^{27}Al and ^{71}Ga in NMR spectra exists for δ as is given by[27]

$$\delta(^{27}\mathrm{Al}) = \delta(^{71}\mathrm{Ga}) + 4.50(\pm 4.90)/2.83(\pm 0.10)$$

Taking $\delta(^{71}\mathrm{Ga}) \approx 246$ ppm for LLZO from our work, we calculate 88 ± 5 ppm for $\delta(^{27}\mathrm{Al})$. An ^{27}Al NMR resonance with this chemical shift value has been measured for Al-bearing LLZO.[4,5,7,8] It was assigned to Al^{3+} at the 96*h* site by DFT calculations.[28] This analysis also argues, albeit indirectly, for the presence of Ga^{3+} at 96*h* in $Li_{7-3x}Ga^{3+}{}_xLa_3Zr_2O_{12}$ garnets.

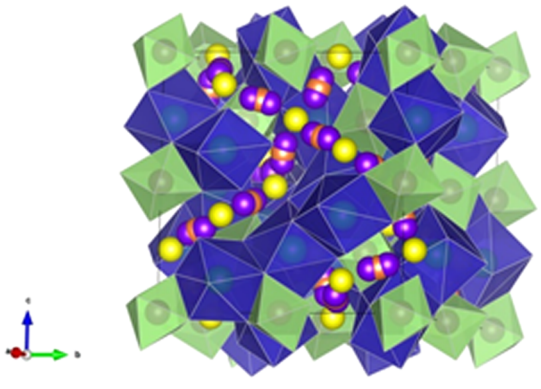

Figure 6. Crystal structure of cubic LLZO. The blue dodecahedrally coordinated sites (24*c*) are occupied by La^{3+} and the green octahedrally coordinated sites (16*a*) by Zr^{4+}. The yellow spheres correspond to tetrahedrally coordinated sites (24*d*), the orange spheres to octahedrally coordinated sites (48*g*) and the purple to "4-fold" coordinated sites (96*h*). These three latter sites can potentially be occupied by Li.

dx.doi.org/10.1021/ic500803h | Inorg. Chem. 2014, 53, 6264−6269

AUTHOR INFORMATION

Corresponding Author

*E-mail: daniel.rettenwander@sbg.ac.at.

Author Contributions

All authors have given approval to the final version of the manuscript.

Funding

The research was supported by Austrian Science Fund (FWF): project number P25702.

Notes

The authors declare no competing financial interest.

ACKNOWLEDGMENTS

We thank M. Fechtelkord (Bochum) for taking the NMR spectra and J. F. Stebbins (Stanford) for helpful discussions on them. M. Wilkening (Graz) kindly read the manuscript and recommended a couple of modifications. We also thank M. Schuhmann for supportive activities.

REFERENCES

(1) Murugan, R.; Thangadurai, V.; Weppner, W. *Angew. Chem.* **2007**, *119*, 7925−7928.

(2) Awaka, J.; Kijima, N.; Hayakawa, H.; Akimoto, J. *J. Solid State Chem.* **2009**, *182*, 2046−2052.

(3) Bernstein, N.; Johannes, M. D.; Hoang, K. *Phys. Rev. Lett.* **2012**, *109*, 205702.

(4) Buschmann, H.; Dölle, J.; Berendts, S.; Kuhn, A.; Bottke, P.; Wilkening, M.; Heitjans, P.; Senyshyn, A.; Ehrenberg, H.; Lotnyk, A.; Duppel, V.; Kienle, L.; Janek, J. *Phys. Chem. Chem. Phys.* **2011**, *13*, 19378−19392.

(5) Geiger, C. A.; Alekseev, E.; Lazic, B.; Fisch, M.; Armbruster, T.; Langner, R.; Fechtelkord, M.; Kim, N.; Pettke, T.; Weppner, W. *Inorg. Chem.* **2011**, *50*, 1089−1097.

(6) Li, Y.; Han, J.-T.; Wang, C.-A.; Vogel, S. C.; Xie, H.; Xu, M.; Goodenough, J. B. *J. Power Sources* **2012**, *209*, 278−281.

(7) Düvel, A.; Kuhn, A.; Robben, L.; Wilkening, M.; Heitjans, P. *J. Phys. Chem. C* **2012**, *116*, 15192−15202.

(8) Hubaud, A. A.; Schroeder, D. J.; Key, B.; Ingram, B. J.; Dogan, F.; Vaughey, J. T. *J. Mater. Chem. A* **2013**, *1*, 8813−8018.

(9) Rangasamy, E.; Wolfenstine, J.; Sakamoto, J. *Solid State Ionics* **2012**, *206*, 28−32.

(10) Kanamura, K.; Kaeriyama, A.; Honda, A.; Yoshida, T.; Sato, Y. US Patent application number 20110053000, 2011.

(11) Kotobuki, M.; Kanamura, K.; Sato, Y.; Yoshida, T. *J. Power Sources* **2011**, *196*, 7750−7754.

(12) Kuhn, A.; Choi, J.-Y.; Robben, L.; Tietz, F.; Wilkening, M.; Heitjans, P. *Z. Phys. Chem.* **2012**, *226*, 525−537.

(13) Jin, Y.; McGinn, P. J. *Electrochim. Acta* **2013**, *89*, 407−412.

(14) Jin, Y.; McGinn, P. J. *J. Power Sources* **2011**, *196*, 8683−8687.

(15) Wolfenstine, J.; Sakamoto, J.; Allen, J. L. *J. Mater. Sci.* **2012**, *47*, 4428−4431.

(16) Tietz, F.; Wegener, T.; Gerhards, M. T.; Giarola, M.; Mariotto, G. *Solid State Ionics* **2013**, *230*, 77−82.

(17) Howard, M. A.; Clemens, O.; Kendrick, E.; Knight, K. S.; Apperly, P. A.; Anderson, P. A.; Slater, P. R. *Dalton Trans.* **2012**, *41*, 12048−12053.

(18) El Shinawi, H.; Janek, J. *J. Power Sources* **2013**, *225*, 13−19.

(19) Skibsted, J.; Nielsen, N. C.; Bildsoe, H.; Jakobsen, H. J. *J. Magn. Reson.* **1991**, *95*, 88−117.

(20) Rettenwander, D.; Geiger, C. A.; Amthauer, G. *Inorg. Chem.* **2013**, *52*, 8005−8009.

(21) Ash, J. T.; Grandinetti, P. J. *Magn. Reson. Chem.* **2006**, *44*, 823−831.

(22) Hellner, E.; Gerlich, R.; Koch, E.; Fischer, W. *Physics Data*; Fachinformationszentrum Energie, Physik, Mathematik: Karlsruhe, Germany, 1979; Vol. *16−1*, pp 1−16.

(23) Allen, J. L.; Wolfenstine, J.; Rangasamy, E.; Sakamoto, J. *J. Power Sources* **2012**, *206*, 315−319.

(24) Geller, S. *Z. Kristallogr.* **1967**, *125*, 1−47.

(25) Cheng, L.; Park, J. S.; Hou, H.; Zorba, V.; Chen, G.; Richardson, T.; Cabana, J.; Russo, R.; Doeff, M. *J. Mater. Chem. A* **2014**, *2*, 172−181.

(26) Shannon, R. D.; Prewitt, C. T. *Acta Crystallogr., Sect. B: Struct. Sci.* **1969**, *B25*, 925−946.

(27) Bradley, S. M.; Howe, R. F.; Kydd, R. A. *Magn. Reson. Chem.* **1993**, *31*, 883−886.

(28) Rettenwander, D.; Blaha, P.; Laskowski, R.; Schwarz, K.; Bottke, P.; Wilkening, M.; Geiger, C. A.; Amthauer, G. *Chem. Mater.* **2014**, *26*, 2617.

NOTE ADDED AFTER ASAP PUBLICATION

After this paper was published ASAP May 29, 2014, a correction was made to reference citations in the last paragraph of the Discussion section. The corrected version was reposted June 3, 2014.